

USV1 IN-FLIGHT LOADS EVALUATION BY MEANS OF STRAIN GAUGE INSTRUMENTATION PART I

L. Di Palma, M. Belardo, N. Paletta, M. Pecora

C.I.R.A. – Italian Aerospace Research Centre
via Maiorise – 81043 Capua (CE)
ITALY

ABSTRACT

The aim of this study is the development of a methodology able to evaluate the flight loads of the Unmanned Space Vehicle 1 (USV1), during the Dropped Transonic Flight Test (DTFT) mission. The USV1 is a multi-mission, re-usable vehicle under development in CIRA, the Italian Aerospace Research Centre. The first USV1 mission is aimed at experimenting the transonic flight of a re-entry vehicle.

The structure experiment will allow achieving two main objectives: validation of design loads and verification of structural design methods. The measurement of external loads during flight will be performed using Skopinski's method. This method is based on the assumption of linear relationships between the direct strain gauge measurements and the external loads (shear and moments). For the first flight this method will be applied only on wing structure.

A set of calibrated strain-gauges has been installed into the vehicle in order to evaluate the main external loads components due to aerodynamic loads.

Preparatory activities have been performed in order to select typology and topology of strain-gauge measurements, to install the onboard sensors, to carry out the ground static calibration for the evaluation of strain/loads transfer functions and to identify the best transfer function.

The choice of strain-gauges typology and topology has been addressed using FE analysis in order to minimize the mutual contaminations between bending, shear and torque outputs. For strain measurements a set of load conditions have been assigned during a static test in the order to encompass as much of the wing span/chord area. A non-conventional and economic device has been developed to punctually apply loads on the wing, transferring only vertical forces. The strain/loads transfer functions have been identified using an automated approach in order to minimize the external loads errors.

It has been found a good agreement between the theoretical loads and the loads evaluated using strain-gauge technique.

1. INTRODUCTION

For a long time, airplane flight loads have been measured using calibrated strain gauges [2]. The first step of such a process consists of determining a linear expression that relates the strain gauges outputs to applied loads during ground load calibration on the lifting surface. The second step is the acquisition of flight data, which involves deducing flight loads from flight-measured strains. The empirical relationships established during the ground load calibration are used in the deductive process.

1.1. An Overview on USV1 Vehicle and DTFT Mission

Italian Aerospace Research Centre is conducting a national research program named USV (Unmanned Space Vehicle). The main objective is designing and manufacturing unmanned Flying Test Beds, conceived as multi-mission flying laboratories, in order to test innovative materials, verify structural and aerodynamic behaviour, advanced guidance, navigation and control (GN&C) functionalities and critical operational aspects typical of the future Reusable Launch Vehicles. The development of such a vehicle requires, in particular, the availability of a number of specific key technologies.

In this framework, a series of missions of increasing complexity has been planned, the first of which is the Dropped Transonic Flight Test (DTFT). The latter is mainly aimed at testing the aerodynamics and flight behaviour in transonic flight regime, in conditions likely to be experienced by a winged launcher stage during its atmospheric re-entry trajectory.

The design of the DTFT is based on using a two-stage system that is composed by an expendable first stage, a carrier based on a stratospheric balloon, and the winged re-entry flight test bed (FTB_1 vehicle), as the second stage. The nominal mission profile of DTFT is schematically depicted in Fig.1 and can be summarised as follows.

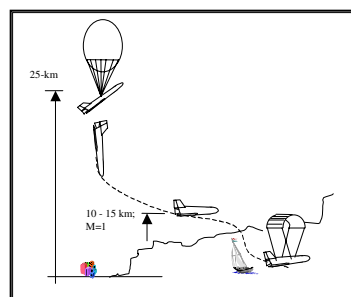


Figure 1. DTFT Mission Scheme

The basic operations consist of three main phases:

1. the ascent phase, from lift-off to the release (around 20 km altitude), during which the carrier system brings the FTB_1 to the release altitude by means of the stratospheric balloon;
2. the flight phase, from vehicle release to parachute opening, where the FTB_1 leaves the carrier and flies accelerating to achieve the required velocity to perform the experiments. In this phase the FTB_1 passes through the transonic regime (Mach number around 1.1), between 10 and 15 km, in stabilized attitude while performing an autonomous aero-controlled flight.
3. the deceleration phase, from parachute opening to splashdown, in which the FTB_1 opens the parachute and ends its mission by sea splashdown and recovery.

The first DTFT was carried out on last 24th February 2007 from Arbatax in Sardegna, Italy.

The vehicle accommodated onboard a scientific payload which was aimed at conducting two main experiments: an aerodynamic test coupled with a structural test for validating the overall aerodynamic and structural design and analysis tools and the GN&C capabilities in terms of analytical results of flight mechanics on stability, manoeuvrability and controllability of the vehicle.

From structural point of view the USV1 have a alluminum alloy multi spars delta wing with low aspect ratio and high swept-back angle as shown in the following scheme.

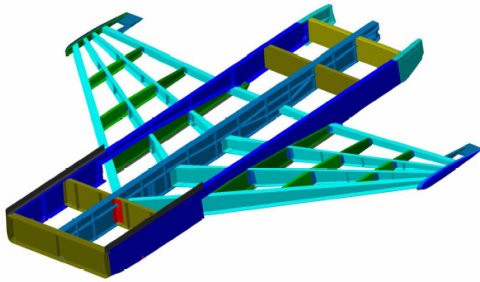


Figure 2. USV1 wing scheme

1.2. Loads Evaluation Equations

The idea of using calibrated strain gauges through influence coefficients formats to measure flight loads on airplane components was perpetuated by Skopinski, Aiken, and Huston in their 1954 report [1]. This flight loads evaluation method is based on the following concept: the relationship between strain, or equivalently stress, and external characteristics shear, bending and torque acting on measurement point is linear. So strain measurements are most commonly developed as a linear combination of load characteristics:

$$(1) \quad \begin{pmatrix} V \\ M \\ T \end{pmatrix}_{FS} = \begin{pmatrix} \beta_{11} & \beta_{12} & \beta_{13} \\ \beta_{21} & \beta_{22} & \beta_{23} \\ \beta_{31} & \beta_{32} & \beta_{33} \end{pmatrix}_{FS} \begin{pmatrix} \mu_1 \\ \mu_2 \\ \mu_3 \end{pmatrix}_{FS}$$

Equations (2) are called "Load equations". V , M , T are respectively Shear, Bending moment and Torque, μ_i

($i=1,2,3$) are three strain gauges measurements in a Fixed Station of the wing, matrix $\underline{\beta}$ is the Transfer Function and its coefficients are determined as follows:

$$(2) \quad \begin{pmatrix} \beta_{11} & \beta_{12} & \beta_{13} \\ \beta_{21} & \beta_{22} & \beta_{23} \\ \beta_{31} & \beta_{32} & \beta_{33} \end{pmatrix}_{FS} = \begin{pmatrix} V_1 & V_2 & V_3 \\ M_1 & M_2 & M_3 \\ T_1 & T_2 & T_3 \end{pmatrix}_{FS} \begin{pmatrix} \mu_{11} & \mu_{12} & \mu_{13} \\ \mu_{21} & \mu_{22} & \mu_{23} \\ \mu_{31} & \mu_{32} & \mu_{33} \end{pmatrix}_{FS}^{-1}$$

Transfer Function $\underline{\beta}$ can be evaluated finding three suitable load conditions (calibration load) and three suitable strain gauge measurements from equations (2). The best transfer function is the one that minimizes errors evaluated as difference between external loads computed by equations (1) and those ones calculated using the concentrated loads applied during ground static calibration test.

The conventional procedure for finding optimum loads and strain gauge measurements combinations to achieve the best transfer function has been well highlighted in some works for no multi-spar and no delta wing. However, with the evolution of supersonic and hypersonic airplanes, this goal has become more complex. In particular, many problems have been resulted for low aspect ratio and delta-wing airplanes [3]. The numerical approach introduced in this paper provides a means of examining the behaviour of load equations for similar load distributions.

2. MATERIALS AND METHODS

In this section the on-board sensors will be reported, moreover the ground static calibration test procedure and the application of Skopinski's methods will be shown for flight loads evaluation of USV1 vehicle.

2.1. On Board Sensors and Instrumentation

Aero-structural experiments make use of two types of sensors acquisitions data: strain-gauge and accelerometers.

The strain-gauge acquisition will be employed in order to qualify structural behaviour of the vehicle and to evaluate the external loads (shear, and moments) in order to validate the theoretical load evaluation methods.

The accelerometers will be employed to identify typical aeroelastic parameters, such as frequency and damping. Approximately 100 strain gauges produced by Vishay Intertechnology Inc. were installed on the vehicle structural items [4].

The evaluation of flight loads has been done for the left semi-wing. It has been divided into three bays and each bay has been monitored by means of four types of strain-gauge bridges. Four monoaxial strain-gauge bridges have been installed on the top and bottom of the spar caps to detect the flexural strain, one arm tri-axial strain-gauge bridge has been mounted on the web spar centerline to detect the pure (or semi-pure) shear deformation and a two arms shear strain-gauge bridge has been mounted on the panel skin. A total of 47 strain-gauges have been installed for loads evaluations.



Figure 3. left semi-wing strain gauges

2.2. Ground Static Calibration Test

The ground calibration test has been carried out applying 9 vertical concentrated forces (C_{ij}) (see APPENDIX A) on left semi-wing at rib-spar intersections as shown in figure 4.

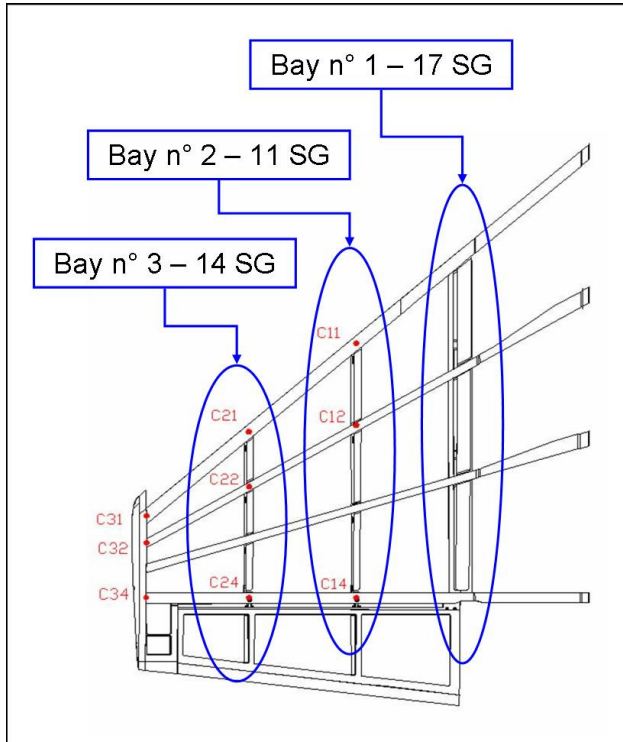


Figure 4. Loading points positions (red) and SG¹ measurements for each bay (blue).

To avoid rigid rotation around roll axis, the vehicle is fixed on three points on a goggle. The wing vertical displacements under each load C_{ij} has been measured by using five analogical dial gauges mounted under wing, as shown in figures 5 and 6.

On the three bays (in correspondence of spar n° 1, 2 and 3), a total of 42 independent strain measurements have

been recorded in order to evaluate the load equations (see APPENDIX B).

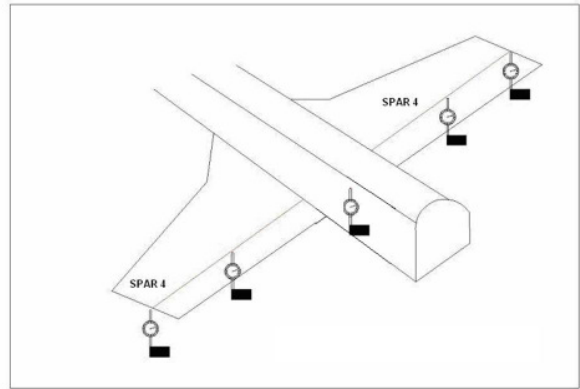


Figure 5. Analogical Dial Gauges positions.



Figure 6. Analogical Dial Gauge mounted under left semi-wing.

2.3. Loads Equations

For load equations determination, the following computational approach has been applied. The transfer functions for all possible combinations of three calibrated forces and three different strain gauge measurements ($\underline{\mu}_{test}$) have been computed using equation (2), then the

external characteristics (\underline{L}_{test}) have been determined applying the following loads equations:

$$(3) \quad \underline{L}_{test} = \underline{\beta} \cdot \underline{\mu}_{test}$$

A series of six load distributions have been defined as a linear combinations of the 9 concentrated loads applied during Ground Calibration Test (see § 2.2, 3.1). These ones have the same chord-wise distribution and differ for spanwise-distribution as shown in figures 7, 8.

¹ SG = Strain-Gauge

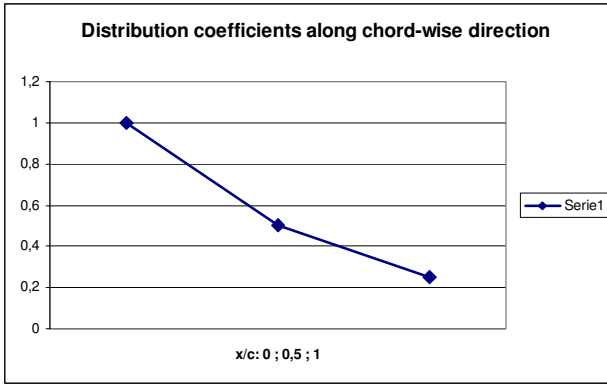


Figure 7. Chord-wise distribution.

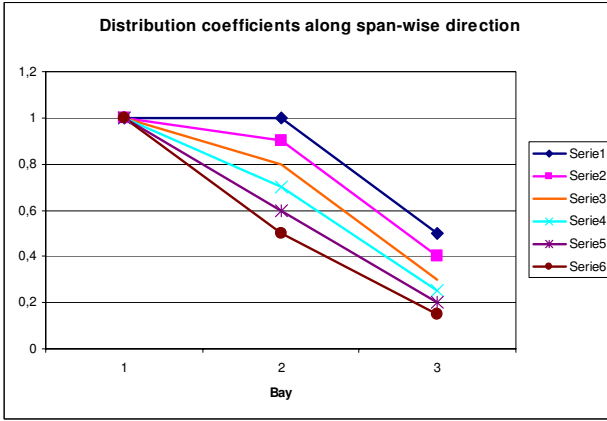


Figure 8. Span-wise distributions.

In a generic bay, the external characteristics due to these six different load distributions are used as comparison load characteristics (\underline{L}_{comp}) for the evaluation of the optimum transfer function ($\underline{\beta}_{opt}$).

For each comparison load, the **Optimum Transfer function** is the one that **minimizes the error** calculated as follows:

$$(4) \quad er = \frac{|\underline{L}_{test} - \underline{L}_{comp}|}{|\underline{L}_{comp}|} \cdot 100.$$

Applying the optimum transfer function associated with i^{st} comparison load ($\underline{\beta}_i$) to homologous strain-gauge measurements ($\underline{\mu}_j$) due to the other comparison loads ($\underline{L}_{comp,j}$), the external loads have been obtained as follows:

$$\underline{L}_{test,ij} = \underline{\beta}_i \cdot \underline{\mu}_j.$$

Finally the coefficients of the “crossed errors” matrix (\underline{CE}) have been calculated as follows:

$$CE_{ij} = \frac{|\underline{L}_{test,ij} - \underline{L}_{comp,j}|}{|\underline{L}_{comp,j}|} \cdot 100.$$

3. RESULTS

For each comparison load and for each bay, the optimum transfer function are evaluated using equation (2). The Minimum errors, the optimum combinations of calibrated forces and the optimum SG measurements are reported in TAB. 1 (for ID of calibrated loads and strain-gauges see APPENDIX A and APPENDIX B).

	Bay 1	Bay 2	Bay 3
	Errors		
Load Distribution 1	1,65	0,53	2,06
Load Distribution 2	0,64	2,16	2,10
Load Distribution 3	2,68	1,14	0,91
Load Distribution 4	1,07	2,06	1,50
Load Distribution 5	1,01	2,10	1,88
Load Distribution 6	1,05	3,61	2,87
	Calibrated Load Cobinations (ID)		
Load Distribution 1	5, 7, 1	1, 8, 2	8, 5, 4
Load Distribution 2	5, 1, 7	9, 1, 2	7, 5, 2
Load Distribution 3	5, 2, 1	6, 1, 8	8, 4, 6
Load Distribution 4	9, 1, 8	9, 6, 1	4, 6, 8
Load Distribution 5	2, 8, 1	4, 3, 1	5, 7, 3
Load Distribution 6	1, 5, 4	2, 1, 9	4, 5, 9
	SG Measurements Cobinations (ID)		
Load Distribution 1	9, 12, 5	3, 10, 4	2, 12, 6
Load Distribution 2	9, 3, 12	1, 4, 10	2, 12, 11
Load Distribution 3	5, 15, 9	4, 10, 2	1, 14, 9
Load Distribution 4	14, 10, 17	4, 2, 10	14, 9, 1
Load Distribution 5	9, 12, 5	1, 10, 6	10, 4, 2
Load Distribution 6	16, 3, 9	2, 10, 4	3, 13, 7

TAB. 1: Optimum parameters for evaluating load equations.

For each bay and each comparison load, the symmetric “difference matrix” $\underline{\Delta}_{LOAD}$ has been defined as follows:

$$\Delta_{LOAD,ij} = \frac{|\underline{L}_{comp,i} - \underline{L}_{comp,j}|}{\frac{|\underline{L}_{comp,i} + \underline{L}_{comp,j}|}{2}} \cdot 100,$$

where

$$\underline{L}_i = \begin{pmatrix} V_i \\ M_i \\ T_i \end{pmatrix}.$$

The coefficients of $\underline{\Delta}_{LOAD}$ are called “dissimilarity loads parameters”.

The aim of the study has been to establish a relationship among crossed errors and dissimilarity loads parameters. In order to hit this target, one can plot the crossed errors with the respect to the components of $\underline{\Delta}_{LOAD}$ for each bay.

The points are fitted applying the least squares method both by linear (in red colour), quadratic (in blue colour)

and cubic (in green colour) curves (see figures 9, 10 and 11).

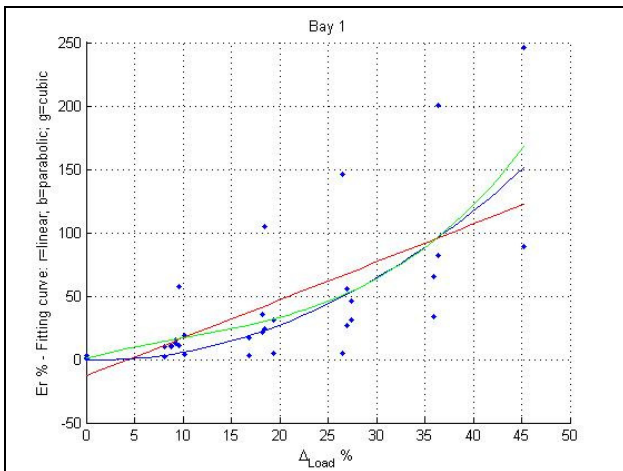


Figure 9. Crossed errors vs dissimilarity loads parameters on bay n^o1.

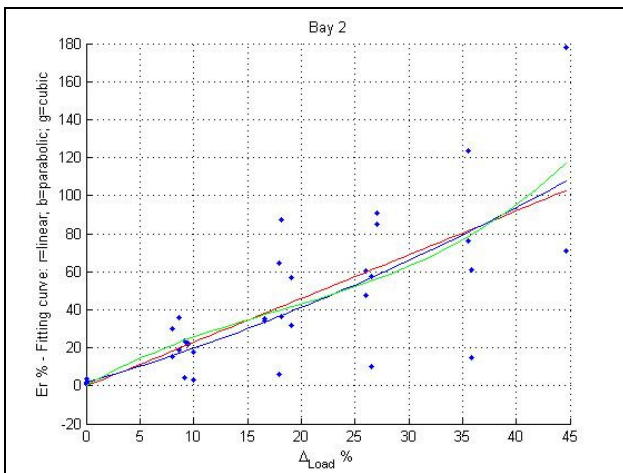


Figure 10. Crossed errors vs dissimilarity loads parameters on bay n^o2.

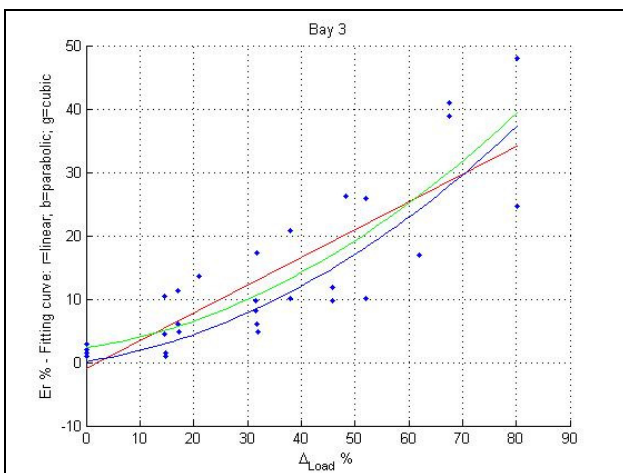


Figure 11. Crossed errors vs dissimilarity loads parameters on bay n^o3.

4. DISCUSSIONS AND CONCLUSIONS

The task of obtaining reliable strain gauge load equations is still complex, even after several decades of experience. Various criteria can be used for evaluating load equations, in this paper a frontal numerical approach has been shown.

Starting from a series of concentrated forces applied during ground calibration test and a set of strain-gauge measurements recorded on each bay, the optimum transfer functions (and load equations) have been computed using equations (2) and (4).

Furthermore, two criteria for determining crossed errors and differences between comparison loads and true external loads have been defined. Figures 9, 10 and 11 highlight a well defined behaviour: if the structure is loaded by a load distribution similar to the comparison load it is possible to determine external characteristics, making an error increasing with the respect to the Dissimilarity Load Parameters in approximately a linear way.

Finally, this study leads to the following conclusions: for flight loads evaluation through SG measurements for DTFT1 mission it needs to apply load equations obtained from comparison loads similar (for chord-wise and span-wise distribution) to expected flight loads. Moreover, it is advisable to validate load equations by further ground calibration tests, carried out by loading the structure with calibration loads as similar as possible to expected flight loads.

5. REFERENCES

- [1] "Calibration of strain-gauge installation in aircraft structures for the measurements of flight loads", NASA Technical Report 1178, T.H. Skopinski, W. S. Aiken Jr and W. B. Huston, 1953
- [2] A Summary of Numerous Strain-Gauge Load Calibrations on Aircraft Wings and Tails in a Technology Format" NASA Technical Memorandum 4804, Jerald M. Jenkins and V. Michael DeAngelis July 1997.
- [3] "A study of the effect of radical load distribution on calibrated strain gauge load equations", NASA-TM-56047, Jerald M. Jenkins and Albert E. Kuhl, July 1977.
- [4] "Consuntivo prova di calibrazione sensori esperimento struttura velivolo FTB_1", CIRA-CF-05-0704, L. Di Palma, November 2005.
- [5] "PRORA USV1: the 1st Italian Experimental Vehicle to the Aerospace Plane", M. Pastena M.P. Di Donato, L. Di Palma; G.Guidotti, L.Pellone, G.Rufolo; R.Sabatano, C.I.R.A., Capua, Italy, 81043 13th AIAA International Space Planes and Hypersonic Systems and Technologies Conference 16-20 May 05

APPENDIX A

In TAB. 2 are reported ID, description and value of all calibrated forces.

ID	Label	Location	Direction	Value [N]
1	C11	Station 1, Spar #1	Vertical	3092
2	C12	Station 1, Spar #2	Vertical	3092
3	C14	Station 1, Spar #4	Vertical	3092
4	C21	Station 2, Spar #1	Vertical	2777
5	C22	Station 2, Spar #2	Vertical	2777
6	C24	Station 2, Spar #4	Vertical	2777
7	C31	Station 3, Spar #1	Vertical	2777
8	C32	Station 3, Spar #2	Vertical	2777
9	C34	Station 3, Spar #4	Vertical	2777

TAB. 2: Calibrated Forces.

APPENDIX B

In TAB. 3, 4 and 5 are reported ID, description and P/N of the analogical dial gauges respectively for bay 1, 2 and 3.

BAY 1		
ID	Description	P/N S. G. VISHAY
1	SG, Left Wing, Spar #1, #1 top	N2A-13T-006N-350
2	SG, Left Wing, Spar #2, #1 top	N2A-13T-006N-350
3	SG, Left Wing, Spar #3, #1 top	N2A-13T-006N-350
4	SG, Left Wing, Spar #1, #1 bot	N2A-13T-006N-350
5	SG, Left Wing, Spar #3, #1 bot	N2A-13T-006N-350
6	SG, Left Wing, Spar #3, #1 bot	N2A-13T-006N-350
7	SG, Left Wing, Spar #1, #1 tri-ax	CEA-13-125-UR-350
8	SG, Left Wing, Spar #1, #1 tri-ax	CEA-13-125-UR-350
9	SG, Left Wing, Spar #1, #1 tri-ax	CEA-13-125-UR-350
10	SG, Left Wing, Spar #2, #1 tri-ax	CEA-13-125-UR-350
11	SG, Left Wing, Spar #2, #1 tri-ax	CEA-13-125-UR-350
12	SG, Left Wing, Spar #2, #1 tri-ax	CEA-13-125-UR-350
13	SG, Left Wing, Spar #3, #1 tri-ax	CEA-13-125-UR-350
14	SG, Left Wing, Spar #3, #1 tri-ax	CEA-13-125-UR-350
15	SG, Left Wing, Spar #3, #1 tri-ax	CEA-13-125-UR-350
16	SG, Left Wing, L S, Spar #2, #1, shear	CEA-06-250-US-350
17	SG, Left Wing, L S, Spar #3, #1, shear	CEA-06-250-US-350

TAB. 3: Analogical Dial Gauge on bay 1.

BAY 2		
ID	DESCRIPTION	P/N S. G. VISHAY
1	SG, Left Wing, Spar #1, #2 top	N2A-13T-006N-350
2	SG, Left Wing, Spar #2, #2 top	N2A-13T-006N-350
3	SG, Left Wing, Spar #3, #2 top	N2A-13T-006N-350
4	SG, Left Wing, Spar #1, #2 tri-ax	CEA-13-125-UR-350
5	SG, Left Wing, Spar #1, #2 tri-ax	CEA-13-125-UR-350

6	SG, Left Wing, Spar #1, #2 tri-ax	CEA-13-125-UR-350
7	SG, Left Wing, Spar #2, #2 tri-ax	CEA-13-125-UR-350
8	SG, Left Wing, Spar #2, #2 tri-ax	CEA-13-125-UR-350
9	SG, Left Wing, Spar #2, #2 tri-ax	CEA-13-125-UR-350
10	SG, Left Wing, Spar #3, #2 tri-ax	CEA-13-125-UR-350
11	SG, Left Wing, Spar #3, #2 tri-ax	CEA-13-125-UR-350

TAB. 4: Analogical Dial Gauge on bay 2.

BAY 3		
ID	DESCRIPTION	P/N S. G. VISHAY
1	SG, Left Wing, Spar #1, #3 top	N2A-13T-006N-350
2	SG, Left Wing, Spar #2, #3 top	N2A-13T-006N-350
3	SG, Left Wing, Spar #3, #3 top	N2A-13T-006N-350
4	SG, Left Wing, Spar #1, #3 tri-ax	CEA-13-125-UR-350
5	SG, Left Wing, Spar #1, #3 tri-ax	CEA-13-125-UR-350
6	SG, Left Wing, Spar #1, #3 tri-ax	CEA-13-125-UR-350
7	SG, Left Wing, Spar #2, #3 tri-ax	CEA-13-125-UR-350
8	SG, Left Wing, Spar #2, #3 tri-ax	CEA-13-125-UR-350
9	SG, Left Wing, Spar #2, #3 tri-ax	CEA-13-125-UR-350
10	SG, Left Wing, Spar #3, #3 tri-ax	CEA-13-125-UR-350
11	SG, Left Wing, Spar #3, #3 tri-ax	CEA-13-125-UR-350
12	SG, Left Wing, Spar #3, #3 tri-ax	CEA-13-125-UR-350
13	SG, Left Wing, L S, Spar #2, #3, shear	CEA-06-250-US-350
14	SG, Left Wing, L S, Spar #3, #3, shear	CEA-06-250-US-350

TAB. 5: Analogical Dial Gauge on bay 3.